Flame retardant study of formalized polyvinyl alcohol fiber coated with melamine formaldehyde resins and the synergistic effect of copper ions

Yan Jiang, Wanli Zhou, Mengjin Jiang, Pengqing Liu, Jianjun Xu

PII: S0141-3910(17)30246-X

DOI: 10.1016/j.polymdegradstab.2017.08.014

Reference: PDST 8325

To appear in: *Polymer Degradation and Stability*

Received Date: 9 June 2017

Revised Date: 27 July 2017

Accepted Date: 11 August 2017

Please cite this article as: Jiang Y, Zhou W, Jiang M, Liu P, Xu J, Flame retardant study of formalized polyvinyl alcohol fiber coated with melamine formaldehyde resins and the synergistic effect of copper ions, *Polymer Degradation and Stability* (2017), doi: 10.1016/j.polymdegradstab.2017.08.014.

Flame retardant study of formalized polyvinyl alcohol fiber coated with melamine formaldehyde resins and the synergistic effect of copper ions

Yan Jiang, Wanli Zhou, Mengjin Jiang, Pengqing Liu,Jianjun Xu*

State Key Laboratory of Polymer Materials and Engineering, College of Polymer Science and Engineering, Sichuan University, Chengdu 610065, China

Abstract: The formalized polyvinyl alcohol fibers (PVF fibers) were grafted with acrylic acids after being activated in dilute potassium permanganate solution, and then the grafted PVF fibers (PVF-g-AA fibers) were reacted with melamine formaldehyde (MF) oligomer solution to form flame-retardant coatings on their surface. The coated PVF fibers (PVF-g-AAMF fibers) were further treated with copper sulfate solution for absorbing copper ions to promote their flame retardant performance. The structure of the fibers was characterized by FTIR spectra and SEM photos. The flame-retardant performance of the fibers was evaluated by limiting oxygen index (LOI) and microcalorimeter tests (MCC tests). It is found that MF coatings effectively improved the flame resistance of PVF fibers, but the flame retardant efficiency was not satisfactory. Copper ions have an obvious synergistic effect on the flame resistance of the fibers. SEM photos of char residues, results of TGA and TG-IR revealed that the flame retardance of MF coatings is mainly due to gaseous phase .The effect of copper ions on the thermal decomposition of MF resins was analyzed with pyrolysis-gas chronograms-mass spectrometry (PyGC-MS), and it is found that copper ions catalyzed the thermal decomposition of MF resins, which synchronized the decomposition of MF resins and PVF fibers. Copper ions are also effective in improving the char residues of PVF-g-AAMF fibers. The flame resistance of the fibers was improved dramatically by the synergistic effect between the grafted MF resin and the copper ions.

Keywords: formalized polyvinyl alcohol fiber; flame resistance; graft polymerization; melamine formaldehyde resin; metal ions; synergistic effect;

1. Introduction

The formalized polyvinyl alcohol fibers (PVF fibers) have been widely used in many areas because of their excellent properties. However, PVF fibers are readily ignitable in the air, and their limiting oxygen index (LOI) is only about 19%. Although, there has been reported a lot of favorable flame retardants (FRs) that can be

---

* *Corresponding author:*
Tel.: +86 02885462013; E-mail address: xujj@scu.edu.cn;
Postal address: Sichuan University, No.24 South Section 1, Yihuan Road, Chengdu, Sichuan 610065, CHINA

used to improve the flame resistance of polyvinyl alcohol (PVA) sheets and membranes. [1-5] Most of those FRs cannot be used for PVA fibers directly because of the rigorous preparation requirement of PVA fibers. As is well known, the as-spun PVA fibers have to be thermal stretched and heat set at about 220°C to improve their crystallinity and orientation degree. Unfortunately, a lot of frequently-used FRs, such as many organo-siloxane FRs, will decompose at this temperature and thus PVA fibers will lose their flame retardancy after heat setting process. [6] Moreover, PVA fibers should be formalized to improve their resistance to hot water before being used in many cases. The formalization process should be catalyzed with the strong acidic environment, which would dramatically affect the structure of many effective FRs, such as melamine polyphosphate (MPP), melamine cyanurate (MCA), ammonium polyphosphate (APP) and most phosphate FRs. Therefore, adopting a post-treatment seems to be an attractive way to avoid these severe process conditions and obtain a flame retardant PVF fiber. Although the post-treatment methods are very convenient and effective, the flame-retardant durability should be taken into account as the flame retardants are easy to be washed away after long-time usage.

In this paper, permanent flame retardant coatings on the surface of PVF fibers were well designed. The PVF fibers were firstly grafted with acrylic acids, and then the carboxyl groups on the surface of the grafted PVF fibers were reacted with the melamine formaldehyde (MF) resin. As a result, the flame retardant coatings were finally formed on the surface of PVF fibers.

MF resin and its derivatives are always considered to be excellent flame retardant materials, and also have been widely used in many applications. [7-9] In our previous work, the MF resin and PVA composite fibers were prepared by wet spinning. [10] The obtained composite fibers were found to be self-extinguishing in the air when the content of MF resins is over 50%, i.e. The flame retardant efficiency of MF resins is not very high. So, it is interesting to investigate if the surface coating technic could make MF resin more efficient in flame retarding PVF fibers.

Moreover, the transition metal ions (such as Cu^{2+}, Ca^{2+} and Zn^{2+}) have been reported owning effective flame resistant effects to acrylic fibers, alginic acid fibers, viscose fibers, etc. [11-17] However, the synergistic effect of metal ions and MF resins has seldom been reported. Therefore, it is also worthwhile to study the synergistic effect of metal ions and MF resins.

In the present work, PVF fibers coated with MF resin were further treated in copper sulfate solution for absorbing copper ions to promote their flame retardant performance. The synergistic effect between copper ions and MF resin was studied in details.

2. Experimental

2.1 Materials

Potassium permanganate, concentrated sulfuric acid (≥98%), formaldehyde aqueous solution (≥37%), melamine, triethylamine, glacial acetic acid and copper sulfate pentahydrate (all from Ke Long Co., Ltd., Chengdu, China), were analytically pure and used as received. Acrylic acid (AA), also purchased from Ke Long Co., Ltd., was analytically pure and used after removing inhibitor. Formalized polyvinyl alcohol

(PVF) fiber, a commercial product, whose acetylation degree was about 25%-30%, was kindly provided by Sichuan Vinylon Works, SINOPEC, Chongqing, China.

2.2 Preparation of Acrylic Acid Grafted PVF fibers (PVF-g-AA fibers)

The acrylic acid grafted PVF (PVF-g-AA) fibers were prepared according to the method described in many reports [18, 19], as is shown in Scheme 1. PVF fibers were firstly immersed into the 0.05 mol L^{-1} potassium permanganate solution at 40°C for 10 min to generate free radicals on their surface. The solid-liquid ratio of the reaction system was 1:40. Then, the activated PVF fibers were washed with de-ionized water until the washing water became colorless. After squeezing out extra water, the activated PVF fibers were immersed into an aqueous acrylic acids solution (concentration: 20 wt%) at 50°C for different times in a nitrogen atmosphere. Sulfuric acid was added into the system to initiate the grafting reaction, and the concentration of sulfuric acid in the reaction system was 0.08 mol L^{-1}. The solid-liquid ratio of the grafting reaction system was 1:80. PVF-g-AA fibers were finally obtained after washing and drying. The grafting degree was calculated according to the following formula:

$$G=(M_t-M_0)/M_0\times 100\%$$

M_o and M_t are the weight of the fibers before and after grafting, respectively.

Scheme 1 The initiation reaction of dilute potassium permanganate solution

2.3 Preparation of MF resin Coating PVF Fibers (PVF-g-AAMF fibers)

The prepolymer of MF resin was synthesized according to the method used in our previous work. [5, 10] Melamine, formaldehyde solution and distilled water were added into a 500 ml three-necked flask at 80°C. The molar ratio of melamine to formaldehyde was 1:2 and the solid content of the system was 5%. Triethylamine was added to the solution to adjust the pH of the system to 9-10. The reactants were stirred until the products became homogeneous, and then the reaction continued for 12 hours to obtain transparent homogeneous MF prepolymer solutions.

PVF-g-AA fibers were then put into the prepared MF prepolymer solutions at 80°C for 1h. The reaction between carboxyl groups which came from the surface of PVF-g-AA fiber and MF prepolymer is shown in Scheme 2. Then, glacial acetic acid was added into the reaction system to adjust the pH of the system under 6, and in that situation, MF prepolymer started to crosslink. After curing for 1 hour, the fibers were taken out and washed with much water to remove the physically adsorbed MF resins. The mass fraction of MF resins was calculated as follows:

$$W=(m_2-m_1)/m_2\times 100\%$$

$m_1$and m_2 are the weight of the fibers before and after reacting with MF resins, respectively.

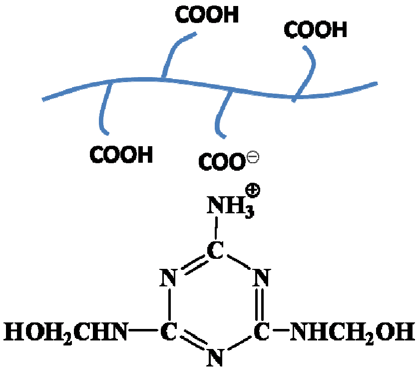

Scheme 2 The proposed reaction between carboxyl groups and MF resins

2.4 Absorbing Copper Ions (PVF-g-AAMFCu fibers)

PVF-g-AAMF fibers were immersed into the 0.50 mol L^{-1} aqueous solution of copper sulfate for 1h at 80°C. The solid-liquid ratio of the reaction system was 1:40. Then, the fibers were washed with hot water for several times to remove the residual copper sulfates. The proposed structure of the PVF-g-AAMFCu fibers is shown in Scheme 3.

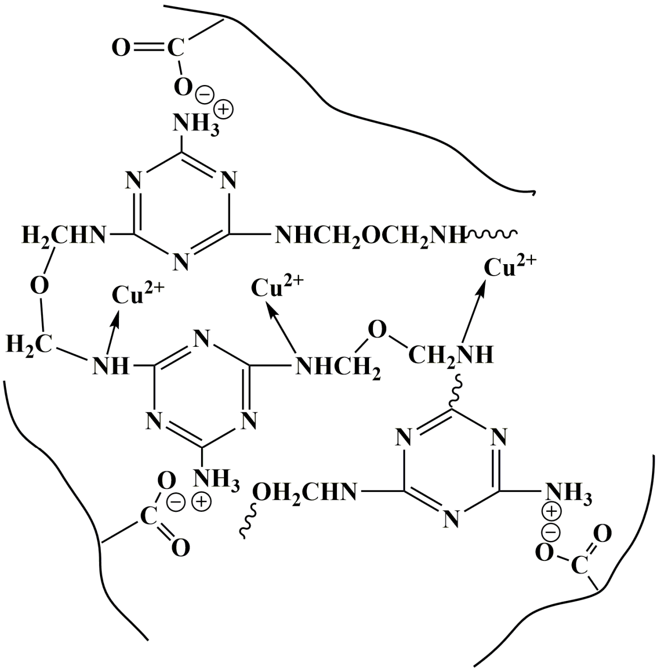

Scheme 3 The proposed structure of PVF-g-AAMFCu fibers

2.5 Preparation of Model Flame Retardants (MFCu resins)

MF resin powders were immersed into the 0.50 mol L^{-1} aqueous solution of copper sulfate for 1h at 80°C. The solid-liquid ratio of the reaction system was 1:40. Then, the MF resins chelated with copper ions (MFCu resins) were finally obtained after washing with hot water for several times in the process of filtration.

2.6 Experimental Techniques

Infrared spectra were recorded using a Nexus-560 (Nicolet, USA) Fourier transform infrared spectrophotometer (FTIR) on fibers powder by transmittance methods. The wave number resolution was 2 cm^{-1}, and the scan region was from 4000 cm^{-1} to 400 cm^{-1}.

The LOI values were measured on an LOI analyzer (Model JF-3, Jiangning Co., China) according to ISO 4589-2. An average of at least five replicas was adopted.

Scanning electron micrographs of the combustion residue were obtained by a JSM-5900LV scanning electron microscope (JEOL). The accelerated voltage was 20 kV.

Thermal gravimetric analysis (TGA) was carried on a TA instrument Q600. The fiber samples were cut into powder and dried in a vacuum oven at 80°C for 12 hrs. The measured temperature was varied from 100°C to 700°C at a heating rate of 10 °C min^{-1} under a nitrogen atmosphere or synthetic air condition.

Thermal gravimetric analysis/infrared spectrometry (TG-FTIR) was performed to analyze the volatilized products after the pyrolysis of samples under a nitrogen flow of 35.0 mL min^{-1}. All samples were approximately 10 mg and were kept at 100°C for 5 min first to remove the absorbed water, then were heated up to 700°C at a heating rate of 10 °C min^{-1}.

The microcalorimetry (MCC) tests were conducted on an FTT0001 microcalorimeter instrument (FTT, UK). The dried powdered fiber samples, placed in a 40 μL alumina crucible, were heated from 100°C to 750°C at a heating rate of 1 °C s^{-1} in a stream of nitrogen flowing at 80 mL min^{-1}. Then, the mixer of the volatile anaerobic thermal degradation products and nitrogen gas stream was mixed with a 20 mL min^{-1} stream of oxygen gas before entering to a 900°C combustor.

The content of copper ions absorbed by the fibers was determined by an ICPS-8100 inductively coupled plasma emission spectrometer (Shimadzu, Japan). The samples were immersed in the concentrated sulfuric acid for 48h at 25°C with stirring so that all the metal ions of the samples were replaced by H^+ and released to the solution. Then, the content of copper ions in the acid solution was tested by ICP.

Scanning electron micrographs (SEM) of the samples were obtained by a JSM-5900LV scanning electron microscope (JEOL). The accelerated voltage was 20 kV.

Pyrolysis-gas chronograms-mass spectrometry (PyGC-MS) was performed on a PY-2020is pyrolysis apparatus (Frontier, Japan) coupled with a GC-MS-QP2010 gas chromatograph/mass spectrometer (Shimadzu, Japan). The samples were pyrolyzed under selected temperature for 12s, and the pyrolysis products were separated and identified by gas chromatograph/mass spectrometer.

3. Results and Discussion

3.1 Structural Characterization

3.1.1 FTIR Spectra

Figure 1 is the FTIR spectra of PVF, PVF-g-AA and PVF-g-AAMF fibers. The broad peak around 3415 cm^{-1} is the stretching vibration absorption of –OH and the peaks at 2942 cm^{-1} and 2862 cm^{-1} are due to the stretching vibration of $–CH_2–$ in the molecular chain. After being grafted with acrylic acids, there appears a strong peak at 1725 cm^{-1}, the characteristic absorption peak of C=O of carboxylic groups, which indicates the successfully grafting of acrylic acids. The peaks at 1585 cm^{-1} and 1488 cm^{-1} of figure 1c are attributed to the in-plane bending vibration of triazine rings of MF resins and the peak at 1332 cm^{-1} is the stretching vibration absorption of C–N, besides, the peak at 811 cm^{-1} is the out-of-plane bending vibration of triazine rings of MF resins. From the results of the FTIR spectra, it can be concluded that the fibers were grafted with acrylic acids and covered with MF resins successfully.

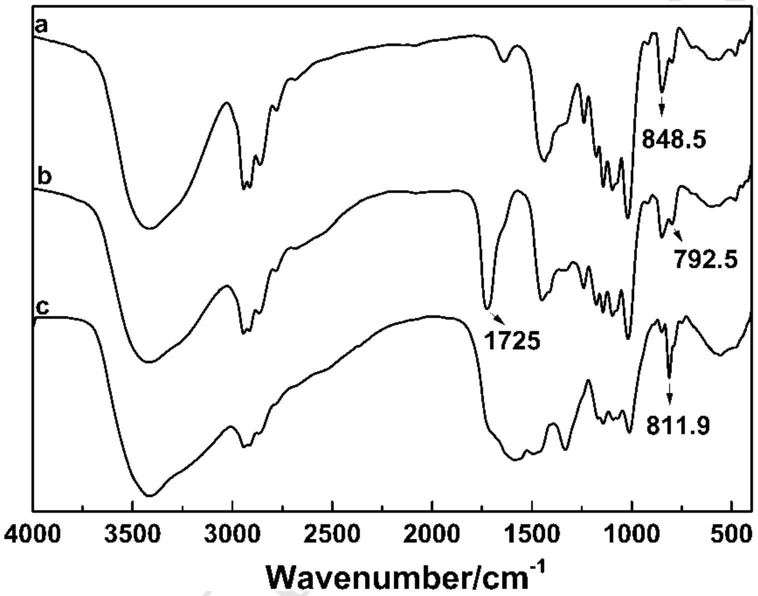

Figure 1 The FTIR spectra of PVF (a), PVF-g-AA (b) and PVF-g-AAMF (c) fibers

3.1.2 SEM Photographs

SEM was used to observe the morphology of the fibers before and after modification, and the results are shown in Figure 2. It can be seen that the surface of PVF fibers is very smooth and the cross-section is compact from inside and out. After being grafted with acrylic acids, the surface of the fibers is still quite smooth, as is shown in Figure 2c. However, compared with the cross-section of PVF fibers, there appears a loose external surface after grafted, which indicates that acrylic acids were grafted on the surface of the PVF fibers. Moreover, this thin outer layer becomes much thicker after reacted with MF resins (Figure 2f) and the surface of the fibers becomes rough (Figure 2e). We can easily get the conclusion that the compact interior section of PVF-g-AAMF fiber is PVF substrate and the loose outer layer is the specially designed flame-retardant coating.

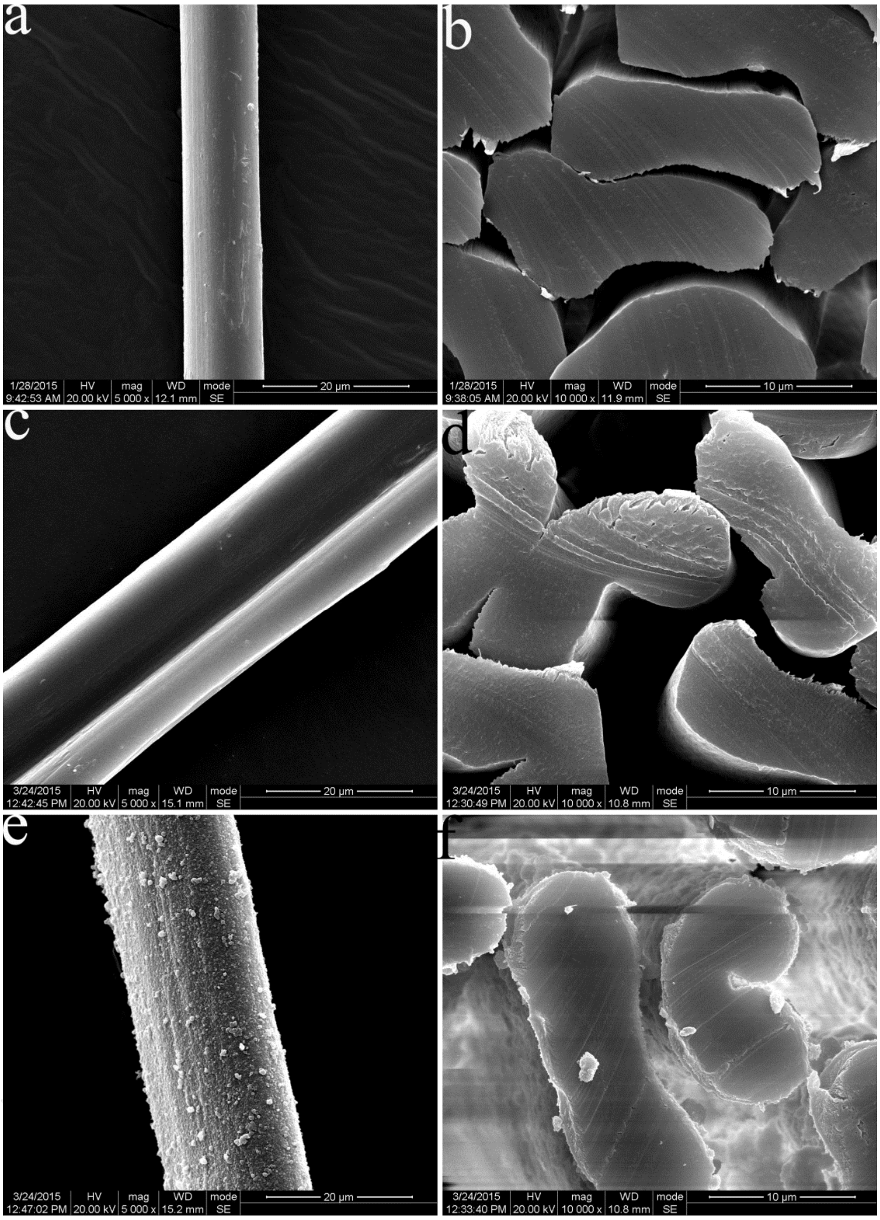

Figure 2 SEM photographs of the surface and cross-section of the fibers; (a-b): PVF fiber; (c-d): PVF-g-AA fiber; (e-f): PVF-g-AAMF fiber

3.2 Flame Resistance of PVF-g-AAMF Fibers

The LOI values of a series of PVF-g-AAMF fibers grafting with MF resins at different degree were tested and the results are shown in Figure 3. The initial LOI value of PVF fibers is only about 19.0% which means PVF fibers burn easily in the air. After grafting with acrylic acids and then coating by MF resins, the LOI value improves significantly. Moreover, it can be seen that the LOI values of PVF-g-AAMF fibers improve rapidly with the increasing of grafting degree at the very beginning. However, with the further increasing of grafting degree, the LOI values of the fibers improve slowly. The flame resistance of PVF-g-AAMF fiber is supposed to depend on its MF coatings. The content of MF resins versus grafting degree is also tested to verify this assumption, and the results are also shown in Figure 3. It can be found that the growth trend of MF resins is similar to that of LOI values as expected. PVF fibers without grafting any acrylic acids can not react with MF resins. As a result, the protective MF coatings can not be formed on their surface. However, after grafting, the carboxyl groups on the surface of the PVF-g-AA fibers will react with MF resins to form the protective coatings. At the beginning stage, the protective MF coatings will become thick with the increasing of acrylic acids, so the content of MF resins and LOI values increased. However, with the further increasing of acrylic acids, the reaction between MF resins and the inner acrylic acids may become harder and blocked, so the content of MF resins and LOI values grow slowly at last. Unfortunately, result from this slow growth of LOI versus grafting degree, the grafting degree should be above 30.0% to obtain the flame resistant fiber (LOI>27%). However, a little increase of grafting degree and the content of MF resins will lead to a sharp decrease in the mechanical properties of the fibers.

PVF-g-AAMF fibers were treated with an aqueous solution of copper sulfate to absorb copper ions and improve the flame retardant efficiency of MF coatings, The LOI values of the PVF-g-AAMFCu fibers are also shown in Figure 3. It can be seen that copper ions can improve the LOI values of PVF-g-AAMF fibers significantly. For example, for PVF-g-AAMF fibers grafting acrylic acids at a degree of 5.1%, the LOI of the fibers increases from 22.0% to 30.8% after absorbed with Cu^{2+}, which is even higher than that of the untreated PVF-g-AAMF fibers grafting acrylic acids at a degree of 58.0%. This remarkable synergistic effect largely promotes the flame retardant efficiency of MF coatings. As a consequence, the needed grafting degree to obtained flame-resistant fibers is dramatically reduced. Although the higher grafting degree will give the fibers thicker MF coatings and better flame resistance, taking the decrease of mechanical properties of fibers with high grafting degree and MF resins contents into account, the grafting degree is preferably below 20%.

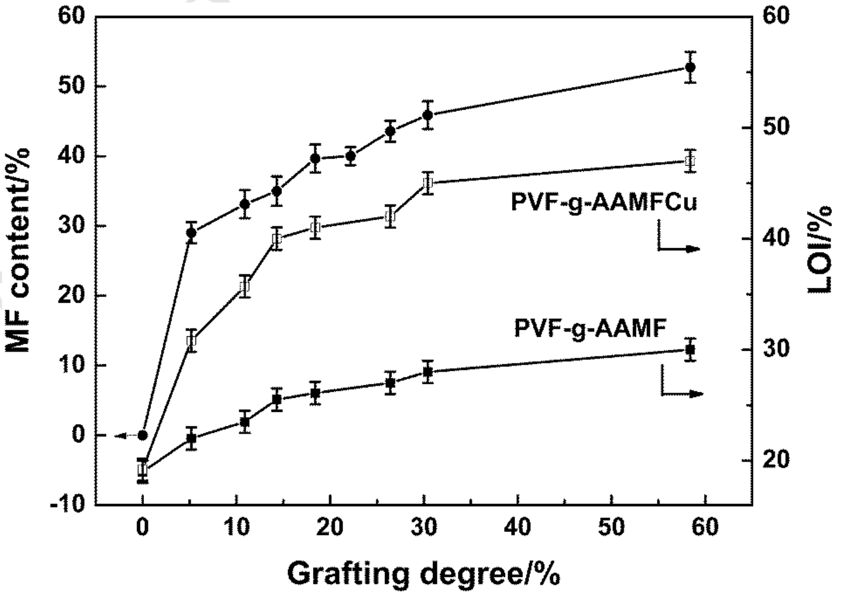

Figure 3 The MF content and LOI values of PVF-g-AAMF fibers versus grafting

degree

3.3 Heat Release Behavior

MCC test is a useful method to investigating the combustion properties of polymer materials. Results include peak heat release rate (pHRR), total heat release (THR) and temperature at the peak heat release rate (T_{max}). Figure 4 presents the curves of the heat release rate of PVF, PVF-g-AA, PVF-g-AAMF and PVF-g-AAMFCu fibers, and the corresponding experimental data are summarized in Table 1.

It can be inferred from Figure 4 that PVF fibers create much more combustible products during heating and HRR reaches a sharp peak with a pHRR of 190.4 W g^{-1}, and pHRR is slightly reduced after grafting with acrylic acids. After covering with MF resins, the pHRR decreases remarkably to 99.7 W g^{-1}, indicating that MF coatings are effective to reduce the heat release rate. Furthermore, the pHRR of PVF-g-AAMFCu fibers is reduced to only about 48.3 W g^{-1}, illustrating that the copper ions lead to a dramatically decreasing of the heat release rate and have an obviously synergistic flame retardancy effect.

THR is characterized as the total energy released by combusting the gasses generated in the process of material decomposition, which is another important parameter for fire hazard evaluation. The data listed in Table 1 show that the THR value of PVF fibers is 18.9 kJ g^{-1} and it reduces to 15.3 kJ g^{-1} after the fiber grafting with acrylic acids, indicating that the combustible gasses generated by acrylic acids during heating are less than that of PVF fiber. It also can be found from Table 1 that the THR of PVF-g-AAMF fiber is about 11.9 kJ g^{-1}. Namely, THR of PVF-g-AA fibers drops 22.2% after coating with MF resins. However, the content of MF resins of the tested PVF-g-AAMF fibers is 35.0±2.1%, implying that the decrease of THR is simply attributed to the introducing of MF resins and MF resins can not enhance the formation of char to prevent the generation of combustible gasses. Therefore, the flame-retardant effect of MF resins may be mostly due to the gaseous phase rather than condensed phase. However, the THR value further decreases to 6.4 kJ g^{-1} after absorbing Cu^{2+}. The much lower THR value of PVF-g-AAMFCu fibers compared with PVF-g-AAMF fibers demonstrates that copper ions have the effect on promoting the content of char residue charring process, thereby preventing the generation of combustible gases during heating. [2]

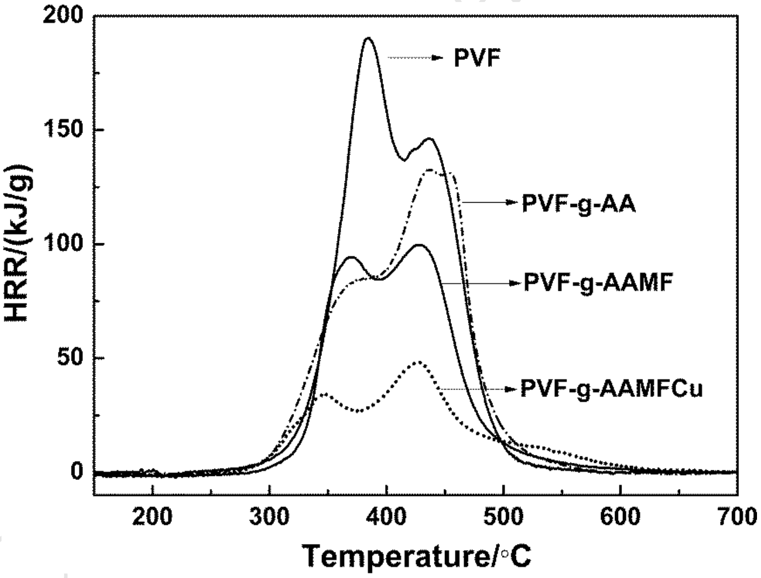

Figure 4 The HRR curves of PVF, PVF-g-AA, PVF-g-AAMF and metal ions treated PVF-g-AAMF fibers

Table 1 MCC test parameters

Sample	$pHRR_1$[a] /(W g^{-1})	$pHRR_2$[b] /(W g^{-1})	THR /(kJ g^{-1})	T_{max1}[c] /(°C)	T_{max2}[d] /(°C)

PVF	190.4	145.7	18.9	384	433
PVF-g-AA	83.2	132.7	15.3	369	437
PVF-g-AAMF	94.4	99.7	11.9	369	429
PVF-g-AAMFCu	34.1	48.3	6.4	345	427

a: The first peak of heat release rate; b: The second peak of heat release rate; c: Temperature at the first peak of heat release rate; d: Temperature at the second peak of heat release rate.

3.4 Thermal Properties

As is well known, the combustion process is very complicated, materials undergo thermal degradation and thermal oxidative degradation processes during burning. [20] Therefore, TGA measurements can serve as useful indicators of polymer flammability. [21, 22] The thermal gravimetric (TG) curves of PVF, PVF-g-AA, PVF-g-AAMF and PVF-g-AAMFCu fibers tested in a nitrogen atmosphere and air atmosphere are shown in Figures 5 and 6, respectively. And the corresponding information of TGA results is also summarized in Tables 2 and 3. Figure 5 shows clearly that the thermal degradation process of PVF fibers can be divided into two stages. It is well known that polyvinyl alcohol dehydrates at the beginning of thermal decomposition process and generates unsaturated compounds. [23, 24] Therefore, the weight loss of the first stage from approximately 318°C to 400°C is related to degradation and elimination of volatile products. When the further increase of the temperature, the main chains start to break down and produce a lot of volatile products and a few char residues finally. Compared to PVF fibers, PVF-g-AA fibers exhibits earlier initial weight loss (T_{on}, the temperature at 5% weight loss) and lower thermal stability below 400°C (decreased T_{max1}) in a nitrogen atmosphere. It may result from the unstable carboxyl groups of acrylic acids which are very easy to eliminate water and carbon monoxide/dioxide during heating. However, T_{max2} of PVF-g-AA fibers is close to that of PVF fibers, which may due to the energy needed to break the molecular chain of PVF and PVF-g-AA fibers down are nearly the same.

It also can be found from Figure 5 and Table 2 that PVF-g-AAMF fibers show almost the same thermal stability with that of PVF-g-AA fibers at the first decomposition stage (the identical T_{on} and T_{max1}) and the weight loss below 360°C is mainly due to the decomposition of the interior acrylic acids. As we can see from Table 4, MF resins are extremely stable [25] under 390℃, and MF resins decompose rapidly at 407℃ and produce some non-flammable gasses and some char residue. However, the char residue of PVF-g-AAMF fiber is only a little higher than that of PVF-g-AA fiber at 800°C, as is given in Table 2. It indicates that the protective effect of MF coating is non-durable and MF coatings can not increase the content of the char, so it can be inferred that the flame retardance of PVF-g-AAMF fiber may be mostly provided by the effect of gaseous phase rather than condensed phase, which is consistent with the results of MCC test.

After further absorbing copper ions, the T_{on} and T_{max1} of the fibers reduce significantly, as is shown in Table 2. Namely, the PVF-g-AAMFCu fiber begin to decompose earlier at first stage, which reveals that copper ions have impacts on catalyzing the degradation of PVA-g-AAMFCu fiber. The *thermostability* of

PVA-g-AAMFCu fiber is different with that of PVF-g-AA fiber. The presence of copper irons with flame-retardant MF resins and acrylic acids, PVF fiber seemed to convert alkylperoxy radicals to more stable species. They strongly affect the extent of carbon formation from and of oxygen uptake by polyolefin molecules as a result of reactions occurring mainly in the condensed phase, enhancing the polymer flame-retardant action. Moreover, the thermal decomposition rate is also further reduced after absorbing copper ions and results in the large increase of char residues. The char residue of PVF-g-AAMF fibers at 800°C significantly increases from 17.2% to 34.4% after absorbing Cu^{2+}. Table 2 also lists the content of copper ions in PVF-g-AAMFCu fibers detected by ICP and the corresponding theoretical calculating char residue of PVF-g-AAMFCu fibers. It can be seen that the theoretical calculating char residue of PVF-g-AAMFCu fibers should be from 16.3% (Cu_2O) to 23.2% (CuO), which is much lower than the measured value (34.4%). Therefore, it can be speculated that the gaseous phase and condensed phase both have an important function in protecting the fibers from burning.

It also can be found from Figure 6 that the thermal stability of PVF and PVF-g-AA fibers below 400°C in air condition are much lower than that of themselves in nitrogen condition (the lower T_{on} and T_{max1}). However, the T_{on} and T_{max1} of PVF-g-AAMF are unchanged no matter heating in air condition or nitrogen condition, which may because MF coatings are very stable in air condition and so can prevent oxygen getting into the interior of the fiber. Therefore, the substrates of PVF-g-AAMF fibers (PVF-g-AA fiber) still undergo thermal decomposition rather than thermal oxidative decomposition even in an air atmosphere. Although MF coating improves the thermal stability of PVF-g-AA fibers significantly in air condition, it can not highly promote the formation of char residue, as is shown in Figure 6, i.e., the barrier action of MF coatings is non-persistent and will be exhausted at high temperature after MF coatings begin to decompose. Thus, it can be inferred that the flame retardant effect of MF resins is mostly based on the gaseous phase and may be with some positive effect of condensed phase, as has been mentioned above.

Notably, the stability of PVF-g-AAMF fibers in nitrogen and air conditions are reduced after absorbing copper ions, declaring that copper ions catalyze the decomposition of PVF-g-AAMF fibers. It can be seen clearly from the DTG curves of figure 6 that the two decomposition stages of PVF-g-AAMFCu fibers coincide with that of PVF fibers. Therefore, the gaseous phase flame retardant effect of PVF-g-AAMFCu fibers is much better than that of PVF-g-AAMF fibers.

It can be drawn from above that copper ions improve the flame resistance of PVF-g-AAMF fibers by improving both the effect of gaseous phase and condensed phase.

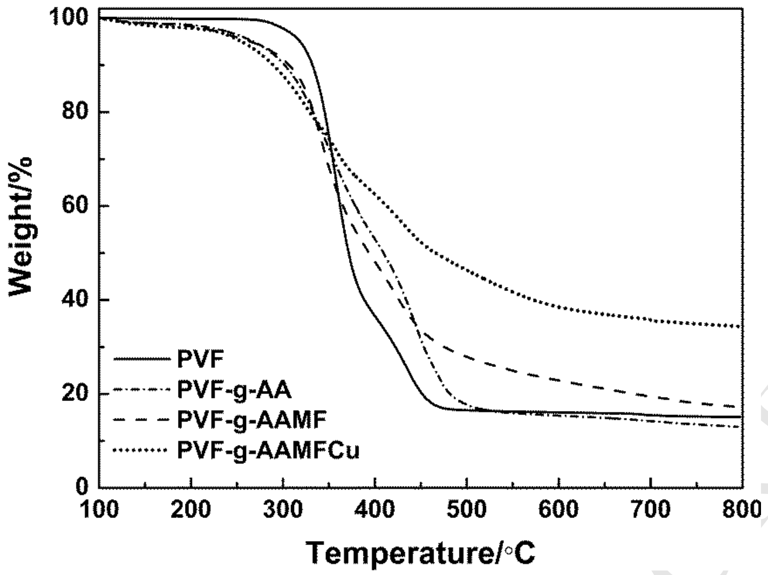

Figure 5 TG curves of PVF, PVF-g-AA, PVF-g-AAMF and PVF-g-AAMFCu fibers tested in nitrogen atmosphere

Table 2 TG Data of PVF, PVF-g-AA, PVF-g-AAMF and PVF-g-AAMFCu fibers tested in nitrogen atmosphere

Sample	T_{on}[a]/(°C)	T_{max1}[b]/(°C)	T_{max2}[c]/(°C)	Char/(%, 800°C)	Content of Cu^{2+}[d]/%	Char[e]/(%, cal.)
PVF	318	358	433	15.1	—	—
PVF-g-AA	267	349	440	13.0	—	—
PVF-g-AAMF	265	342	421	17.2	—	—
PVF-g-AAMFCu	254	323	430	34.4	5.61	16.3-23.2

a: Temperature of 5% weight loss; b: The maximum-rate degradation temperature of the first stage; c: The maximum-rate degradation temperature of the second stage; d: Detected by ICP; e: Calculated char residue, Char (cal.) =5.61% Char (Cu^{2+}) + 94.39% Char (PVF-g-AAMF).

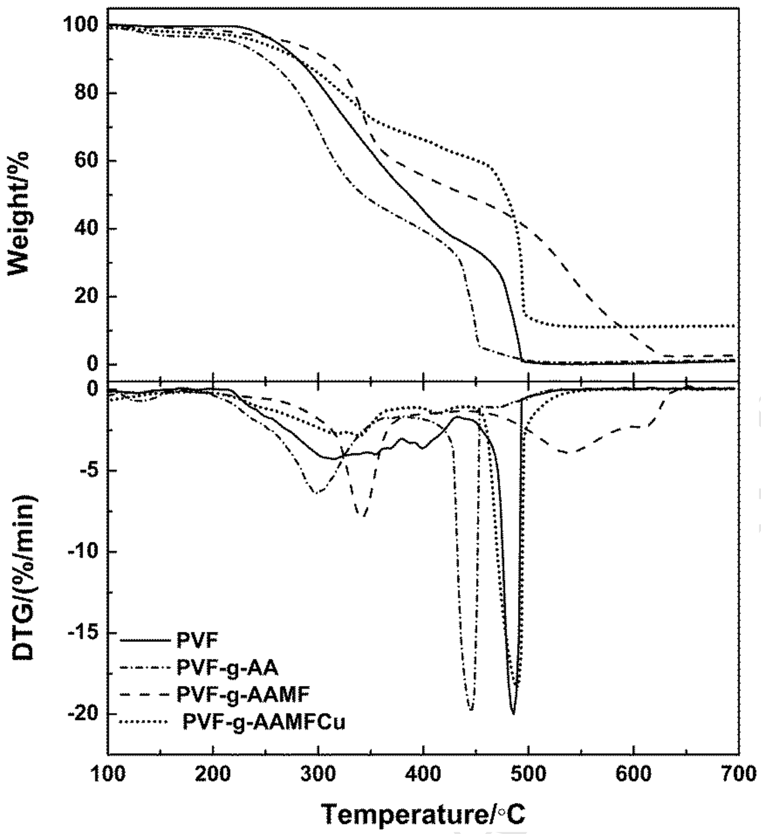

Figure 6 TG and DTG curves of PVF, PVF-g-AA, PVF-g-AAMF and PVF-g-AAMFCu fibers tested in air condition

Table 3 TG Data of PVF, PVF-g-AA, PVF-g-AAMF and PVF-g-AAMFCu fibers tested in air atmosphere

Sample	T_{on}^{a}/(°C)	T_{max1}^{b}/(°C)	T_{max2}^{c}/(°C)	Char/(%, 800°C)	Char^{d}/(%, cal.)
PVF	258	316	486	0.7	—
PVF-g-AA	221	298	445	1.3	—
PVF-g-AAMF	273	341	537	2.7	—
PVF-g-AAMFCu	244	342	488	11.4	8.9-9.6

a: Temperature of 5% weight loss; b: The maximum rate degradation temperature of the first stage; c: The maximum rate degradation temperature of the second stage; Calculated char residue;

3.5 Carbon Residue Morphology

PVF-AAMF and PVF-g-AAMFCu fibers are burned on an alcohol blast burner in the air, and the char residues of the fibers are collected and analyzed to clarify the combustion behavior of the fibers, The SEM photos of the char residue are shown in Figure 7. PVF and PVF-g-AA fibers burn rapidly with much smoke after being ignited by blast burner, and almost no carbon residue is produced, so Figure 7 only gives the char residues of PVF-g-AAMF and PVF-g-AAMFCu fibers. It can be found that the residues of both PVF-g-AAMF and PVF-g-AAMFCu fibers almost completely retains the fibrous structure after burning in air, which may because the low concentration of oxygen in the air makes partial fibers decompose without the participation of oxygen during burning. It also can be seen from Figure 7a that PVF-g-AAMF fibers appear a lot of bumps after burning, which may because MF coatings obstruct the escape of volatile gasses produced by the inner substrates during heating. The bumps of PVF-g-AAMFCu fibers, however, are much fewer and smaller than that of PVF-g-AAMF fibers, as is shown in Figure 7b. It can be well explained by the lower volatile gasses produced during heating, which has been confirmed by MCC tests and TGA results.

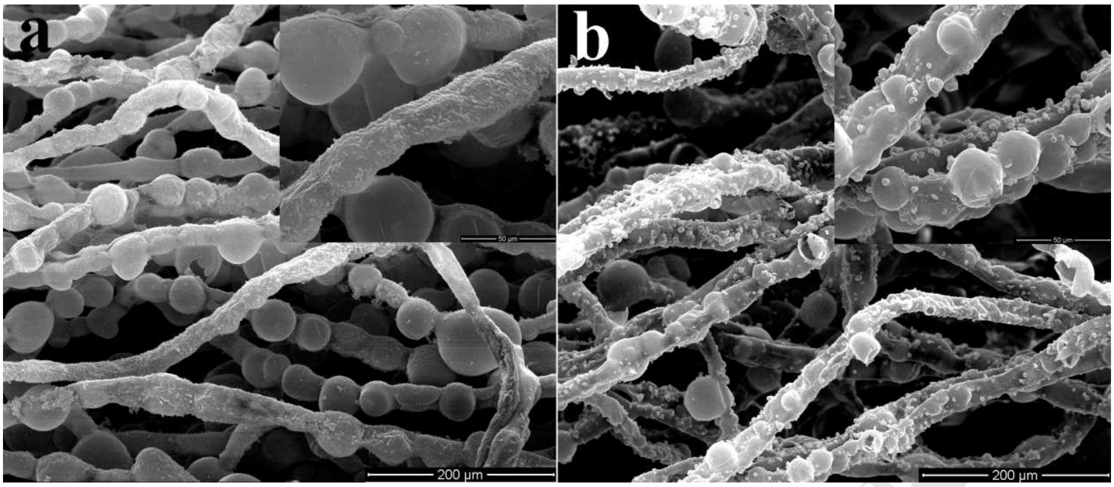

Figure 7 The SEM photos of the char residues of PVF-g-AAMF (a) and PVF-g-AAMFCu (b) fibers collected after burning in air

3.6 Volatilized Products Analysis

Thermal gravimetric analysis/infrared spectrometry (TG-FTIR) technique was applied to study the flame-retardant mechanism in the gaseous phase, and the results are shown in Figures 8 and 9. The FTIR spectra of the volatile gasses generated by PVF fiber at different pyrolysis temperature are shown in Figure 8a. It can be found that a large amount of volatile gases are generated during heating and the main volatile gases are carbon dioxide (2358 cm^{-1}, 2320 cm^{-1} and 669 cm^{-1}), carbon monoxide (2178 cm^{-1} and 2112 cm^{-1}), formaldehyde (2822 cm^{-1}, 2726 cm^{-1} and 1745 cm^{-1}), water (3565 cm^{-1}), aromatic compounds (1560 cm^{-1}, 1540 cm^{-1} and 1508 cm^{-1}), carbonyl compounds (1716 cm^{-1}), methyl compounds (2932 cm^{-1} and 2860 cm^{-1}) and methylene compounds (2895 cm^{-1}, 2861 cm^{-1} and 1470 cm^{-1}). The absorption peaks of the volatile gasses released by PVF-g-AA fibers during heating are shown in figure 8b, almost the same with that of PVF fibers. It can be easily comprehended that all the pyrolysis gases of PVF and PVF-g-AA fibers besides carbon dioxide and water are combustible, which results in the high flammability of PVF and PVF-g-AA fibers. It also can be seen from Figure 8c that the absorption peaks of the combustible gasses are very weak after being covered by MF resins. Simultaneously, there are also much ammonia (965cm^{-1} and 930 cm^{-1}), hydrogen cyanide (3333 cm^{-1}, 3272 cm^{-1} and 714 cm^{-1}) and isocyanic acid (2251 cm^{-1}, 2284 cm^{-1}). Ammonia is supposed to be nonflammable and is a favor to improve the flame retardancy of the fibers. Therefore, the flame resistance of the fiber is improved for higher content of nonflammable gasses and lower content of combustible gasses are generated during heating. The peak intensities of combustible gasses are further reduced after absorbing copper ions, as is shown in Figure 8d, and the peak intensities of ammonia are improved at the same time, which results in the higher flame retardant efficiency.

Some specific volatilized products, including carbon dioxide (2358 cm^{-1}), formaldehyde (1745 cm^{-1}), carbonyl compounds (1716 cm^{-1}), methyl compounds (2932 cm^{-1}), methylene compounds (2895 cm^{-1}), ammonia (965 cm^{-1}), hydrogen cyanide (714 cm^{-1}) and isocyanic acid (2284 cm^{-1}) are selected to study for revealing their changes at different temperature and the results are shown in Figure 9. The intensities of absorbance were all normalized to the samples' content. Figure 9a shows the peak intensities of the volatile gasses produced by PVF fibers at different temperatures. It can be seen that PVF fibers begin to decompose at about 260°C with the release of formaldehyde and carbonyl compounds, which declaring that the cross-linked structure formed during acetylation process is not stable and easy to be destroyed at relatively low temperature. Carbon dioxide can be detected from about

340°C, meaning hydroxyl groups on side chains start to decompose at that temperature. Methyl and methylene compounds are mostly generated during the second decomposition stage at about 450°C with the breaking of molecular backbones. It can be found from Figures 9(b-e) that PVF-g-AAMF fibers release CO_2 at very low temperature about 224°C, but the decomposition products of its MF coatings (NH_3, HCN, and HNCO) start to be detected at a relatively high temperature about 350°C. Therefore, it is proved that the weight loss of PVF-g-AAMF fibers occurs at the very beginning, so the flame retardant efficiency of MF coatings is relatively low. Compared to PVF-g-AAMF fibers, PVF-g-AAMFCu fiber generates CO_2 at a relatively lower temperature about 170°C, which may account for the catalytic effects of copper ions on the decomposition of acrylic acids, as has been reported by many researchers. Moreover, NH_3 and HCN begin to be detected at a much lower temperature about 267°C and 300°C respectively, indicating that copper ions also have the effect of catalyzing the decomposition of MF resins. The catalytic effect of copper ions makes the decomposition temperature of MF resins more close to that of PVF fibers and results in a higher flame retardant efficiency. Besides, it also can be found that the amount of NH_3 is highly improved (Figure 9c) after absorbing copper ions, which also helps to improve the flame retardant efficiency.

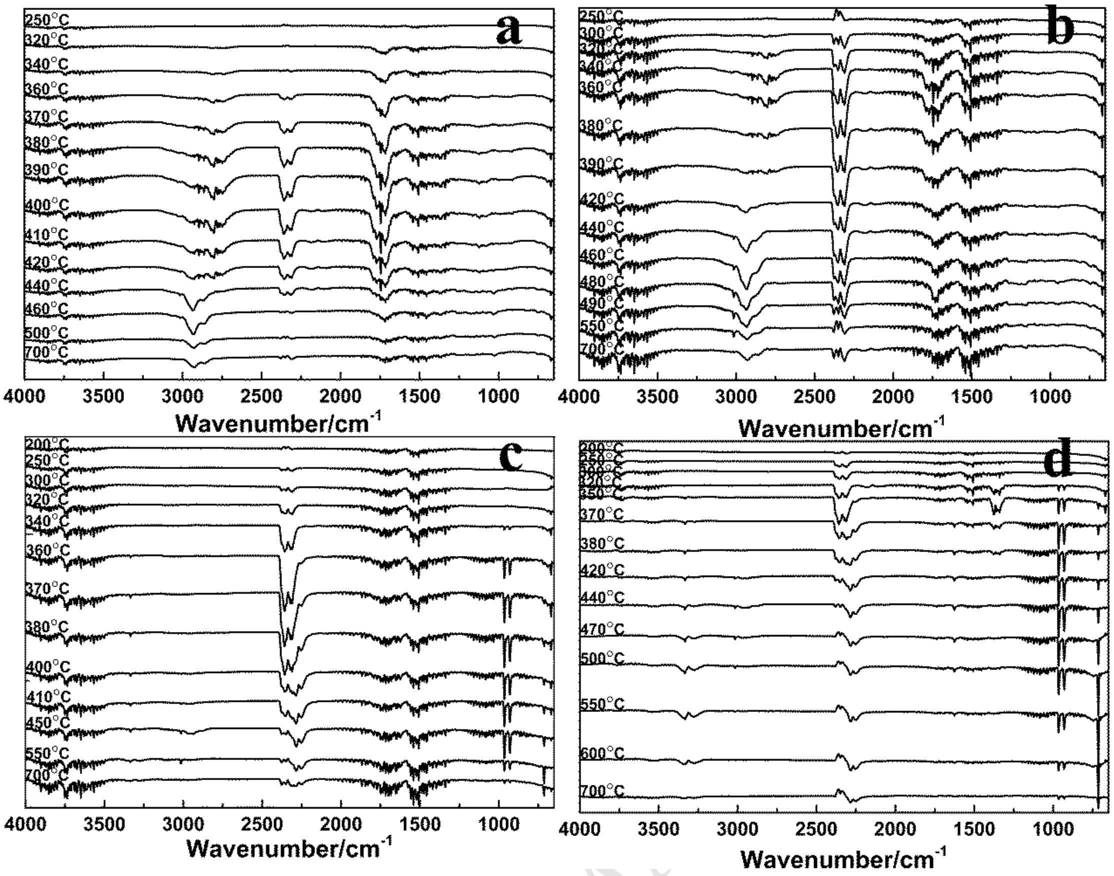

Figure 8 Volatile gasses spectra measured by TG-FTIR for PVF (a), PVF-g-AA (b), PVF-g-AAMF (c) and PVF-g-AAMFCu (d)

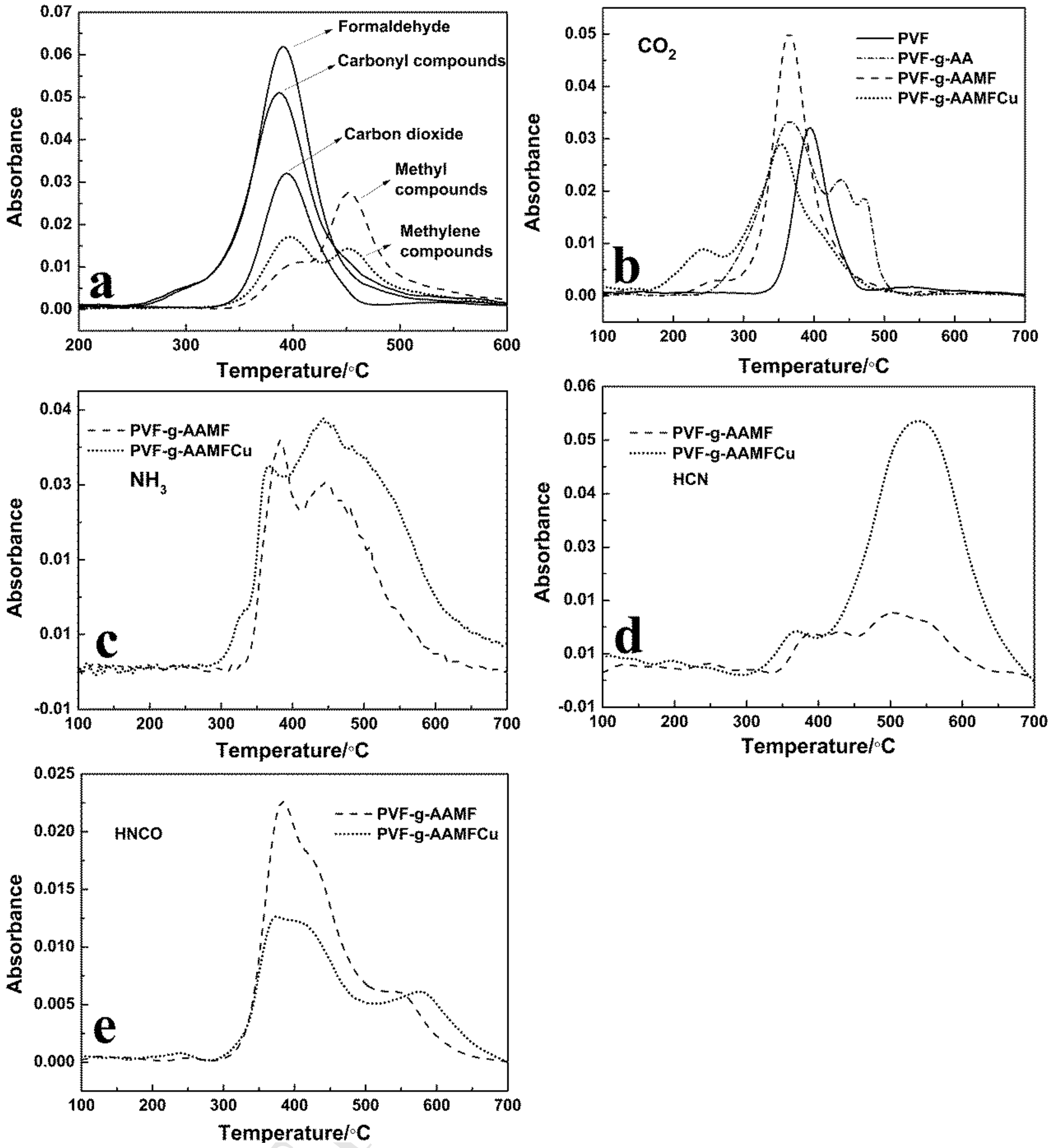

Figure 9 Changes of pyrolysis products at different temperatures. (a): peak intensities of volatile gasses released by PVF fiber at different temperature; (b-e) peak intensities of CO_2, NH_3, HCN and HNCO released by the three kinds of fibers at different temperature, respectively

3.7 XPS analysis of MF and MFCu Resins

X ray photoelectron spectroscopy (XPS) is an analytical technique for characterizing surface elements and their chemical states. The model flame retardants

(MF and MFCu resins) were synthesized, and they were measured by XPS to verify how the Cu^{2+} are absorbed on MF resin, and the results are shown in Figure 10 and Figure 11. Figure 10 a shows the full pattern of MF resin and MFCu resin. Signals at around 288.2 eV, 401.3 eV and 534.5eV corresponding to C1s, N1s, O1s peeks. What's more, there is a new peak of Cu2p arisen at around 950 eV after absorbing Cu^{2+}, and the enlarged image was shown in Figure 10 b.The signals at around 938.2eV and 944.7eV in are peaks of Cu2p$_{1/2}$ and Cu2p$_{3/2}$ which reveals the presence of Cu^{2+}. In Figure 11, there is only one single signal at around 398.5 eV which is assigned to the N1s peak of MF resin for all the nitrogen atoms are in a large conjugated system and the chemical environment of them are the same. After absorbing Cu^{2+}, the peak of N1s can be separated into two peaks. The peak at 399.5 eV is assigned to the coordinate bonds between Cu^{2+} and the N atoms in –NH– groups. And the peak at 398.2 eV is assigned to the C–N bonds in three triazine rings. Because of the strong coordinate bonds, Cu^{2+} can exist stably in PVF fiber and helps to improve the flame retardant efficiency.

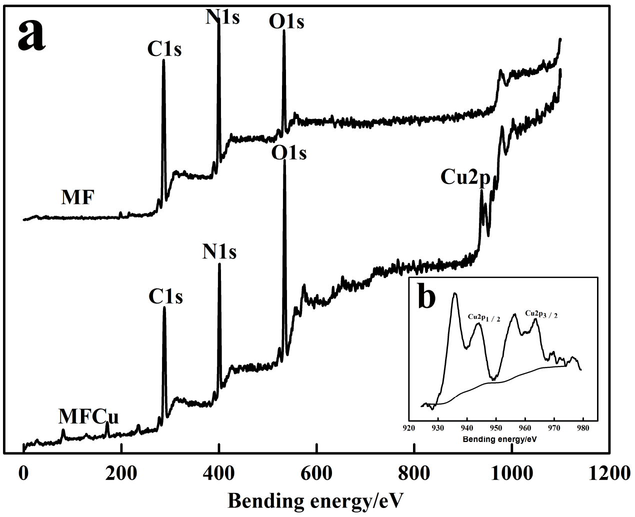

Figure 10 XPS spectra of (a) MF resins and MFCu resins, (b) Cu2p of MFCu resins

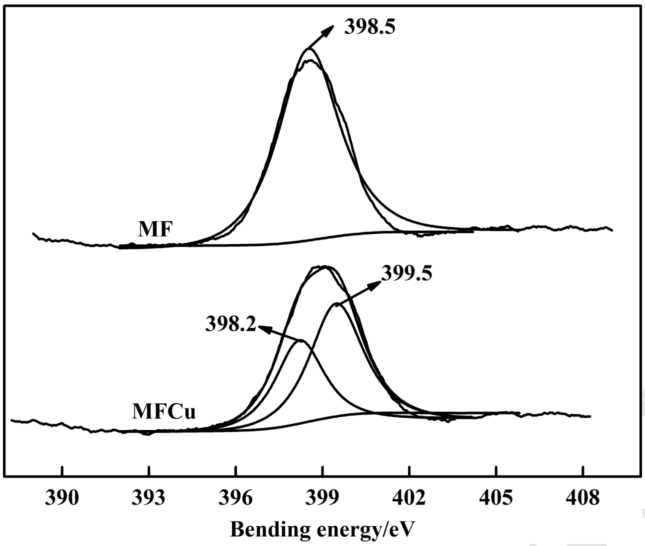

Figure 11 XPS spectra of MF resins and MFCu resins: N1s

3.8 Thermal Properties of MF and MFCu Resins

The model flame retardants (MF and MFCu resins) were synthesized, and their thermal stability was measured by TGA to verify the effect of copper ions on catalyzing the decomposition of MF resins, and the results are shown in Figure 12 and Table 4. It is clearly that the thermal stability of MF resins is largely reduced after being absorbing copper ions. The first decomposition stage of MF resins is from 390°C to 445°C, which is much higher than that of PVF fibers (318°C to 402°C). Comparatively, the first decomposition stage of MFCu resins is reduced to the range from 307°C to 390°C, which is even lower than that of PVF fibers. Therefore, the flame retardant efficiency is largely improved after absorbing copper ions.

It also can be seen that the char residues of MF and MFCu resins from 450°C to 700°C is nearly the same, indicating that copper ions can not improve the char residues of MF resins. However, it has been proved above that copper ions improved the char residues of PVF-g-AAMF fiber, as is shown in Figure 5. It may due to copper ions improve the char residues of acrylic acids. The influence of metal ions on the thermal degradation of acrylic acids has been studied and reported in many reports, and it was found that copper ions have the effect of improving the char residues of acrylic acids and also can catalyze acrylic acids degrade at a lower temperature simultaneously. [27]

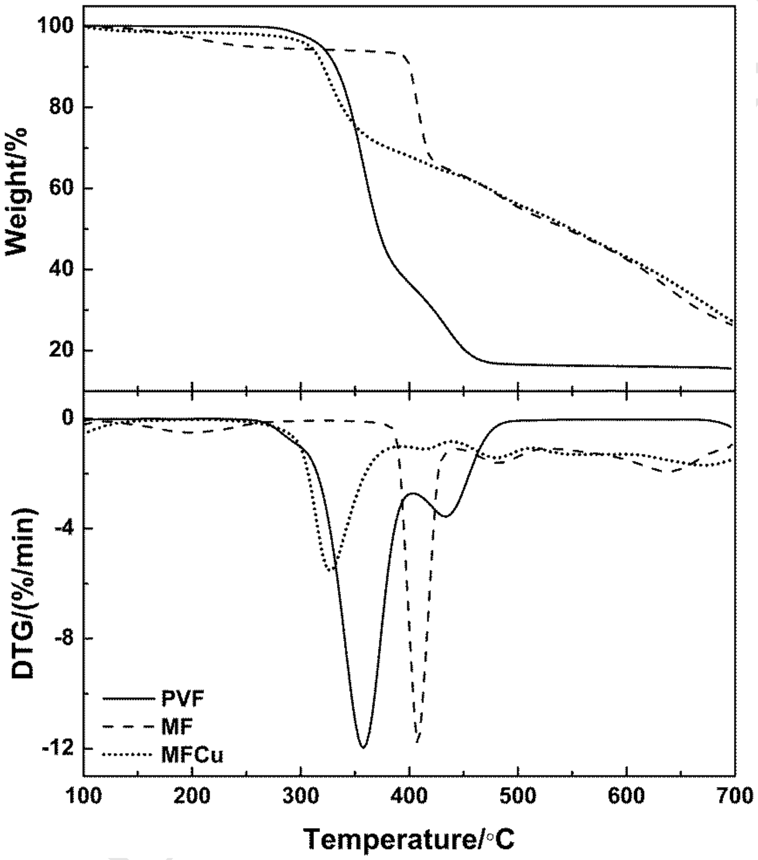

Figure 12 TG and DTG curves of PVF fiber, MF and MFCu resins tested under nitrogen condition

Table 4 TG Data of PVF, MF and MFCu tested in nitrogen atmosphere

Sample	T_{on}^{a}/(°C)	T_{max1}^{b}/(°C)	T_{max2}^{c}/(°C)	Char/(%, 700°C)
PVF	318	358	433	15.1
MF	390	407	—	26.3

MFCu	307	327	—	27.3

a: Temperature of 5% weight loss; b: The maximum rate degradation temperature of the first stage; c: The maximum rate degradation temperature of the second stage;

3.9 Pyrolysis Gas Chromatography/Mass Spectrometry

PyGC-MS was used to analyze the pyrolysis products of MF and MFCu resins at different temperatures. The main products of the two resins are given in Tables 5 and 6, respectively. It can be seen that methanamide is one of the main products of the two resins, which may because HCHO and NH_3 can not be separated by gas chromatography and the radicals of them generated in mass spectrometer reacted with each other and then formed a large amount of methanamide. From the results of PyGC-MS and studies of many researchers [28-35], the thermal degradation of MF resin can be depicted in Scheme 4. It also can be found from Tables 5 and 6 that the main products of MF and MFCu resins are almost the same. However, CO_2, HNCO, and R-$NHCH_3$ of MFCu resins are less than that of MF resin, but the content of HCN, HCHO, NH_3 and R-NH_2 are more than that of MF resin. It indicates that copper ions promote the decomposition of $RNHCH_2OCH_2NHR$ in the way of the second route, as is shown in Scheme 4. The hypothetical catalysis effect of copper ions is shown in Scheme 5. The similar conclusions that metal ions can catalyze the thermal decomposition of many polymers also have been reported by a lot of researchers. [36-38]

Table 5 The main pyrolysis products of MF resins at different temperature

Compounds	m/(z)	R.T./(min)	Peak area/(%,

			400°C	440°C)	500°C
CO_2	44	1.643	5.18	8.03	48.69
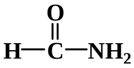 $\mathrm{H{-}\overset{\overset{O}{\|}}{C}{-}NH_2}$	45	1.830	35.75	35.67	—
HNCO	43	6.988	2.37	—	—
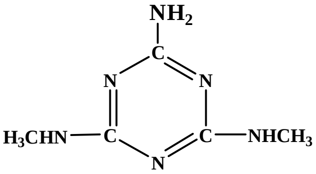	154	15.608	7.29	6.19	—
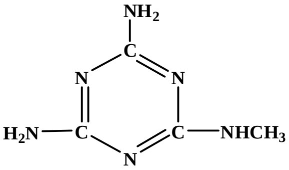	140	15.980	24.93	44.40	35.34
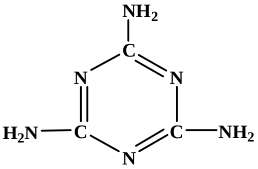	126	16.431	14.5	0.37	1.29
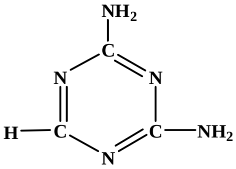	111	13.310	—	4.01	3.55
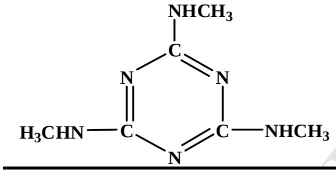	168	15.703	—	—	6.10

Table 6 The main pyrolysis products of MFCu resins at different temperature

Compounds	m/(z)	R.T./(min)	Peak area/(%,		
			310°C	360°C)	420°C
CO_2	44	1.643	—	—	
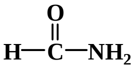 $\mathrm{H{-}\overset{\overset{O}{\|}}{C}{-}NH_2}$	45	1.830	31.21	6.53	17.23

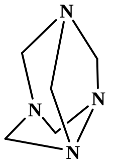	140	11.629	3.44	0.74	0.23
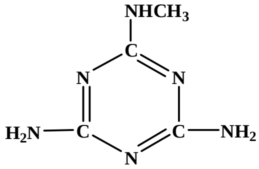	140	15.639	29.16	64.77	63.60
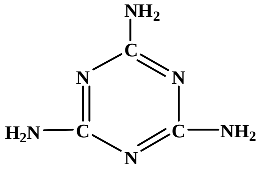	126	16.900	35.40	2.20	1.59
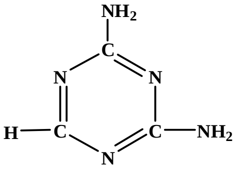	111	13.125	—	3.66	1.99
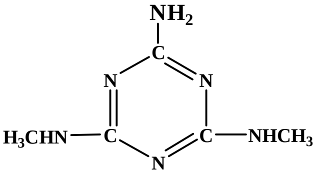	154	15.831	—	7.70	—
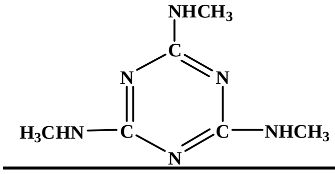	168	15.663	—	4.99	—

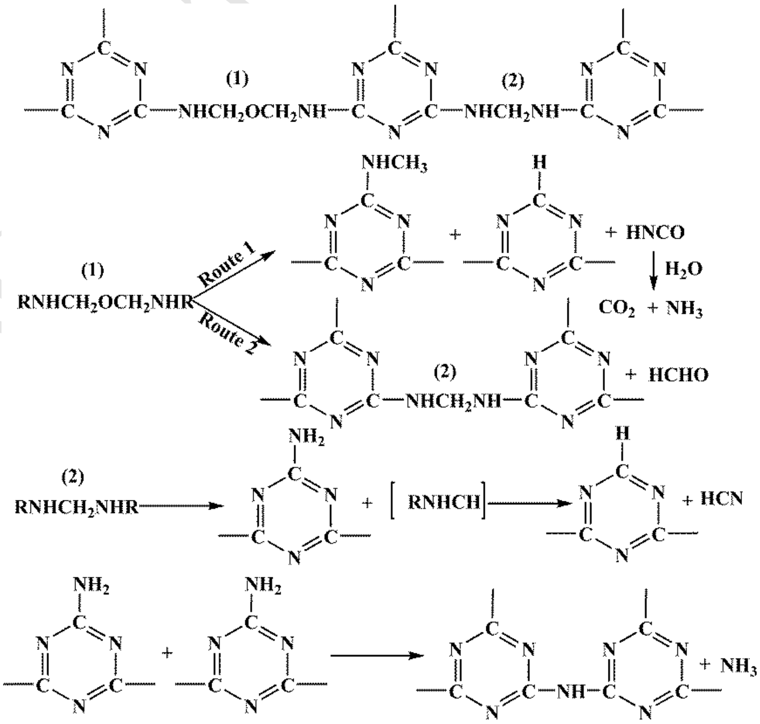

Scheme 4 The supposed thermal degradation of MF resin

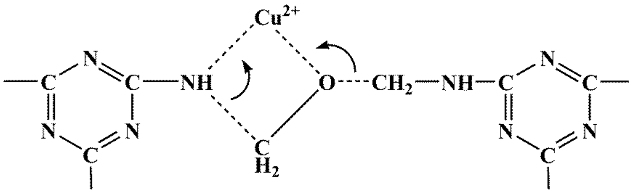

Scheme 5 The hypothetical catalysis effect of copper ions

4. Conclusions

In this paper, PVF fibers coated with MF resins are prepared successfully, and it is found that MF coatings have the effect of improving the flame resistance of PVF fibers. However, the flame retardant efficiency of MF coatings is very low. TG and TG-FTIR results reveal that the low efficiency of MF coatings is mostly due to its very high thermal stability. Fortunately, the flame retardant efficiency is highly improved after absorbing copper ions. It is found that copper ions can catalyze the MF resins to decompose at a relatively low temperature, and it also can promote MF resins to generate more NH_3, which is considered to be helpful to improve the flame resistance. Moreover, copper ions also improve the char residues of the fibers. Therefore, the flame retardant efficiency is finally improved by improving the effect of gaseous phase and condensed phase.

5. Acknowledgement

The authors gratefully acknowledge State Key Laboratory of Polymer Materials and Engineering, College of Polymer Science and Engineering, Sichuan University, China.

References

[1] Wang DL, Liu Y, Wang DY, Zhao CX, Mou YR, Wang YZ. A Novel Intumescent Flame-retardant System Containing Metal Chelates for Polyvinyl Alcohol. Polym Degrad Stabil 2007; 92(8): 1555-1564.

[2] Lu HD, Wilkie CA, Ding M, Song L. Flammability Performance of Poly(vinyl alcohol) Nanocomposites with Zirconium Phosphate and Layered Silicates. Polym Degrad Stabil 2011; 96: 1219-1224.

[3] Hu S, Song L, Pan HF, Hu Y. Effect of a Novel Chitosan-based Flame Retardant on Thermal and Flammability Properties of Polyvinyl Alcohol. J Therm Anal Calorim 2012; 112(2): 859-864.

[4] Feng JX, Zhang XM, Ma SQ, Xiong Z, Zhang CZ, Jiang YH, Zhu J. Syntheses of Metallic Cyclodextrins and Their Use as Synergists in a Poly(Vinyl Alcohol)/Intumescent Flame Retardant System. Ind Eng Chem Res 2013; 52(8): 2784-2792.

[5] Chen WL, Fu XW, Ge WB, Xu JJ, Jiang MJ. Microencapsulation of Bisneopentyl Glycol Dithiopyrophosphate and Its Flame Retardant Effect on Polyvinyl Alcohol. Polym Degrad Stabil 2014; 102: 81-87.

[6] Zhou W, Yang H, Guo X, et al. Thermal degradation behaviors of some branched and linear polysiloxanes[J]. Polymer Degradation & Stability, 2006, 91(7):1471-1475.

[7] Wu WD, Yang CQ. Statistical Analysis of the Performance of the Flame Retardant Finishing System Consisting of a Hydroxy-functional Organophosphorus Oligomer and the Mixture of DMDHEU and Melamine–formaldehyde Resin. Polym Degrad Stabil 2004; 85(1): 623-632.

[8] Yang CQ, Wu WD, Xu Y. The Combination of a Hydroxy-functional Organophosphorus Oligomer and Melamine-formaldehyde as a Flame Retarding Finishing System for Cotton. Fire Mater 2005; 29(2): 109-120.

[9] Salaün F, Lewandowski M, Vroman I, Bedek G, Bourbigot S. Development and Characterisation of Flame-retardant Fibres from Isotactic Polypropylene Melt-compounded with Melamine-formaldehyde Microcapsules. Polym Degrad Stabil 2011; 96(1): 131-143.

[10] Yu CH, Xu WX, Zhao XS, Xu JJ, Jiang MJ. Effects of the Reaction Degree of Melamine-formaldehyde Resin on the Structures and Properties of Melamine-formaldehyde/Polyvinyl Alcohol Composite Fiber. Fiber Polym 2014; 15(9): 1828-1834.

[11] Xu JZ, Tian CM, Ma ZG, Gao M, Guo HZ, Yao ZH. Study on the Thermal Behaviour and Flammability of the Modified Polyacrylonitrile Fibers. J Therm Anal Calorim 2001; 63: 501-506.

[12] Hassan MA, Shehata AB. The Effect of Some Polymeric Metal Chelates on the Flammability Properties of Polypropylene. Polym Degrad Stabil 2004; 85(1): 733-740.

[13] Kong QS, WAng BB, Ji Q, Xia YZ, Guo ZX, Yu J. Thermal Degradation and Flame Retardancy of Calcium Alginate Fibers. Chinese J Polym Sci 2009; 27: 807-812.

[14] Hu S, Song L, Pan HF, Hu Y. Thermal Properties and Combustion Behaviors of Chitosan Based Flame Retardant Combining Phosphorus and Nickel. Ind Eng Chem

Res 2012; 51(9): 3663-3669.

[15] Fang XM, Sun CF, Gao M. Thermal Stability and Smoke Suspension of Cotton Cellulose Modified with Lanthanide Metal Complexes. Combust Sci Technol 2013; 185(7): 1044-1055.

[16] Gao ZH, Yao TT, Ma TF, Tan LW, Xu DM, Ji Q, Xia YZ. Flame Retardant Cellulose Fibers Modified by K$^+$ or Na$^+$. Polym. Mater. Sci. Eng. 2013; 29: 146-158.

[17] Zhou WL, Yan X, Liu PQ, Jiang MJ, Xu JJ. Flame Retardant Modification of Acrylic Fiber with Hydrazine Hydrate and Sodium Ions. J Appl Polym Sci 2015; 132(22): 41996-42005.

[18] Zeng HM, Xu ZD, Lu Y. Investigation of Chelating Fibers . Preparation of Chelating Fiber Containing Amidoxime Group. Ion Exange and Adsorption (Chinese) 1993; 9(3): 216-222.

[19] Tang M, Li SW, Tong Z. Grafting of Acrylicnitril onto Cellulose by Using Mn^{4+}. Basic Sciences Journal of Textile Univerities (Chinese) 2002; 15(3): 220-228.

[20] Bao ZY, Dong YM. Research and Application Intumescent Flame Retardants. Harbin: Harbin Institute of Technology Press. 2005; 8-17.

[21] Cullis CF, Hirschler MM. The Significance of Thermoanalytical Measurements in the Assessment of Polymer Flammability. Polymer 1983; 24(7): 834-840.

[22] Hirschler MM. Thermal Analysis and Flammability of Polymers Effect of Halogen-metal Additive Systems. Eur Polym J 1983; 19: 121-129.

[23] Alexy P, Kachova D, Krsiak M, Bakos D, Simkova B. Poly(vinyl alcohol) Stabilisation in Thermoplastic Processing. Polym Degrad Stabil 2002; 78: 413-421.

[24] Fernandes DM, Hechenleitner AAW, Pineda EAG. Kinetic Study of the Thermal Decomposition of Poly(vinyl alcohol)/Kraft Lignin Derivative Blends. Thermochim Acta 2006; 441(1): 101-109.

[25] Girods P, Dufour A, Rogaume Y, Rogaume C, Zoulalian A. Pyrolysis of Wood Waste Containing Urea-formaldehyde and Melamine-formaldehyde Resins. J Anal Appl Pyrol 2008; 81(1): 113-120.

[26] Pearce EM. Flame Retardants for Polymer Systems. Pure Appl Chem 1986; 58(6): 925-930.

[27] Sebastian N, George B, Mathew B. Metal Complexes of Poly(acrylic acid): Synthesis, Characterization and Thermogravimetric Studies. Polym Degrad Stabil 1998; 60: 371-375.

[28] Anderson IH, Cawley M, Steedman W. Melamine-Formaldehyde Resins II.*-Thermal Degradation of Model Compounds and Resins. Brit Polym J 1971; 3: 86-92.

[29] Manley TR. Characterization of Thermosetting Resins by Thermal Analysis. Journal of Macromolecular Science: Part A - Chemistry 1974; 8(1): 53-64.

[30] Hirata T, Kawamoto S, Okuro A. Pyrolysis of Melamine-Formaldehyde and Urea-Formaldehyde Resins. J Appl Polym Sci 1991; 42: 3147-3163.

[31] Watanabe C, Kawahara Y, Ohtani H, Tsuge S. Development of Pyrolysis-fractography. J Anal Appl Pyrol 2002; 64: 197-205.

[32] Leidl M, Schwarzinger C. Pyrolysis and THM Reactions of Melamine and Its Resins. J Anal Appl Pyrol 2005; 74(1-2): 200-203.

[33] Friedel B, Greulich-Weber S. Preparation of Monodisperse, Submicrometer Carbon Spheres by Pyrolysis of Melamine-formaldehyde Resin. Small 2006; 2(7): 859-863.

[34] Girods P, Dufour A, Rogaume Y, Rogaume C, Zoulalian A. Thermal Removal of Nitrogen Species from Wood Waste Containing Urea Formaldehyde and Melamine Formaldehyde Resins. J Hazard Mater 2008; 159(2-3): 210-221.

[35] Alshehri SM, Al-Fawaz A, Ahamad T. Thermal Kinetic Parameters and Evolved Gas Analysis (TG–FTIR–MS) for Thiourea–formaldehyde Based Polymer Metal Complexes. J Anal Appl Pyrol 2013; 101: 215-221.

[36] Tian CM, Xie JX, Guo HZ, Xu JZ. The Effect of Metal Ions on Thermal Oxidative Degradation of Cotton Cellulose Ammonium Phosphate. J Therm Anal Calorim 2003; 73: 827-834.

[37] Ahamed MAR, Burkanudeen AR. Thiazole-Based Novel Terpolymer Ligand and Its Transition Metal Complexes: Thermal and Biological Studies. Adv Polym Tech 2013; 32(4): 21376-21391.

[38] Ahmad N, Alam M, Alotaibi MAN. Synthesis, Characterization, and Thermal Degradation Kinetics of Biuret–formaldehyde Polymeric Ligand and Its Polymer Metal Complexes. J Therm Anal Calorim 2014; 119(2): 1381-1391.

Figure Captions:

Figure 1 The FTIR spectra of PVF (a), PVF-g-AA (b) and PVF-g-AAMF (c) fibers

Figure 2 SEM photographs of the surface and cross-section of the fibers; (a-b): PVF fiber; (c-d): PVF-g-AA fiber; (e-f): PVF-g-AAMF fiber

Figure 3 The MF content and LOI values of PVF-g-AAMF fibers versus grafting degree

Figure 4 The HRR curves of PVF, PVF-g-AA, PVF-g-AAMF and metal ions treated PVF-g-AAMF fibers

Figure 5 TG curves of PVF, PVF-g-AA, PVF-g-AAMF and PVF-g-AAMFCu fibers tested in nitrogen atmosphere

Figure 6 TG and DTG curves of PVF, PVF-g-AA, PVF-g-AAMF and MF-g-AAMFCu fibers tested in air condition

Figure 7 The SEM photos of the char residues of PVF-g-AAMF (a) and VF-g-AAMFCu (b) fibers collected after burning in air

Figure 8 Volatile gasses spectra measured by TG-FTIR for PVF (a), PVF-g-AA (b), PVF-g-AAMF (c) and PVF-g-AAMFCu (d)

Figure 9 Changes of pyrolysis products at different temperatures. (a): peak intensities of volatile gasses released by PVF fiber at different temperature; (b-e) peak intensities of CO_2, NH_3, HCN and HNCO released by the three kinds of fibers at different temperature, respectively

Figure 10 XPS spectra of (a) MF resins and MFCu resins ,(b) Cu2p of MFCu resins

Figure 11 XPS spectra of MF resins and MFCu resins:(a) N1s

Figure 12 TG and DTG curves of PVF fiber, MF and MFCu resins tested under nitrogen condition

Table captions:

Table 1 MCC test parameters

Table 2 TG Data of PVF, PVF-g-AA, PVF-g-AAMF and PVF-g-AAMFCu fibers tested in nitrogen atmosphere

Table 3 TG Data of PVF, PVF-g-AA, PVF-g-AAMF and PVF-g-AAMFCu fibers tested in air atmosphere

Table 4 TG Data of PVF, MF and MFCu tested in nitrogen atmosphere

Table 5 The main pyrolysis products of MF resins at different temperature

Table 6 The main pyrolysis products of MFCu resins at different temperature